Spectrochimica Acta Part A: Molecular and Biomolecular Spectroscopy 216 (2019) 404–410

Contents lists available at ScienceDirect

Spectrochimica Acta Part A: Molecular and Biomolecular Spectroscopy

journal homepage: www.elsevier.com/locate/saa

Near-infrared fluorescent probe for selective detection of Cu^{2+} in living cells and *in Vivo*

Zhiyang Xu, Hong Wang, Zhen Chen, Hongli Jiang, Yanqing Ge *

School of Chemistry and Pharmaceutical Engineering, Taishan Medical University, Taian, Shandong 271016, PR China

ARTICLE INFO

Article history:
Received 16 November 2018
Received in revised form 19 February 2019
Accepted 18 March 2019
Available online 19 March 2019

Keywords:
NIR
Bioimaging
Fluorescent probe
Cu^{2+}

ABSTRACT

A NIR-rhodamine fluorescent probe was designed and successfully synthesized. The structure of the probe **NRh-Cu** was characterized by ^{1}H NMR, ^{13}C NMR and HRMS. The probe was found to show high sensitivity and high selectivity. The detection limit was calculated to be as low as 0.95 ppb. The sensing mechanism was proposed and confirmed by HRMS spectra. Furthermore, it could be used for imaging Cu^{2+} in living cells and *in vivo*.

1. Introduction

Copper, as an important trace element in the human body, plays a major role in a variety of fundamental physiological processes in organisms ranging from bacteria to mammals [1–3]. However, excessive amount of copper results in liver disease, psychiatric or neurologic symptoms by damaging the liver and nervous system while hematological and neurological disorder such as Menkes disease is reported to be resulted from copper deficiency [4–6]. Hence, it is very important to develop various methods to efficiently detect copper *in vitro* and *in vivo*.

Luminescence bioimaging has attracted great attention in the medical diagnosis and biological analysis [7,8]. Up to now, a large number of fluorescent probes for detection of Cu^{2+} have been reported [9]. However, most of them have relatively short absorption and emission wavelength (UV/Vis), which renders them difficult to be used for sensing and imaging in living animals due to their poor tissue penetration ability [10]. On the other hand, the near-infrared (NIR) fluorophores at around 650–900 nm have many obvious advantages such as the reduction of background absorption, fluorescence, and light scattering. Furthermore, they show good tissue penetration ability with less damage [11–13]. Therefore, it is significant and appealing to develop NIR probes to detect Cu^{2+} *in vivo*. Herein, we report the synthesis, spectroscopic properties, and *in vivo* biological imaging applications of NIR Cu^{2+} probes.

2. Experimental section

2.1. Materials and equipment

UV–vis spectra and fluorescence spectra were recorded on a U-3900 UV–Vis spectrometer and FS 5 luminescence spectrophotometer at room temperature, respectively. ^{1}H NMR and ^{13}C NMR spectra were measured on a Bruker 400 (400 MHz) instrument ($CDCl_3$ as solvent and tetramethylsilane as an internal standard). The mass spectra were recorded on an AB SCIEX 5800 matrix-assisted laser desorption ionization time-of flight mass spectrometer. All reagents and solvents were purchased from commercial sources and used without further purification. The solutions of metal ions were prepared from chlorizated salts which were dissolved in deionized water, and the latter was used throughout the process of absorption and fluorescence determination. The limit of detection (LOD) for the Cu(II) was calculated as 3 times the standard deviation for the average measurements of 10 blank samples by slope (LOD = $3\sigma/K$).

2.2. Cell culture and imaging

The HeLa cell lines were provided by the Institute of Biochemistry and Cell Biology, SIBS, CAS (China). The HeLa cells were cultured in MEM (modified Eagle's medium) supplemented with 10% FBS (fetal bovine serum) at 37 °C and 5% CO_2. Cell images were obtained *via* a confocal microscope from FV1000 (Olympus) at excitation of 630 nm.

* Corresponding author.
E-mail address: geyanqing2016@126.com (Y. Ge).

https://doi.org/10.1016/j.saa.2019.03.062
1386-1425/

2.3. Fluorescence in vivo imaging

Animal procedures were in agreement with the guidelines of the Institutional Animal Care and Use Committee. In this small animal *in vivo* fluorescence imaging system, a 635 nm continuous wavelength laser (Connet Fiber Optics, China) was used as the excitation source, and the fluorescence signal was collected by Andor DU897 EMCCD.

Compounds **1**, **2**, **3** and **5** were synthesized according to the literature [4,14].

2.4. Synthesis of compound ***6***

Compound **3** (0.42 g, 1 mmol) and compound **5** (0.48 g, 1 mmol) were dissolved in acetic anhydride (6 mL), and the reaction mixture was heated to 50 °C and further stirred for 60 min. Then, water (20 mL) was added to the reaction mixture to quench the reaction. The solvent was removed under reduced pressure to give the crude product, which was purified by silica gel flash chromatography using CH_2Cl_2 to CH_2Cl_2/ethanol (0 to 6:1) as eluent to afford compound **6** as a green solid in 65% yield. ^{1}H NMR (400 MHz, $CDCl_3$): δ 8.62 (s, 1H), 8.27 (d, J = 8.0 Hz, 1H), 7.73 (m, 1H), 7.63 (m, 1H), 7.43 (m, 2H), 7.30 (m, 2H), 7.18 (d, J = 8.0 Hz, 2H), 6.74 (d, J = 8.0 Hz, 1H), 6.58 (m, 1H), 6.10 (m, 1H), 4.19 (s, 2H), 3.56 (s, 4H), 2.91 (s, 3H), 2.69 (s, 2H), 2.31 (s, 2H), 1.83 (s, 6H), 1.50 (t, J = 7.2 Hz, 3H), 1.28 (t, J = 7.2 Hz, 6H).

2.5. Synthesis of compound 7

Compound **6** (0.67 g, 1 mmol), hydrazine hydrate (1.00 g, 20 mmol) and BOP Reagent (0.45 g, 1 mmol) were dissolved in CH_2Cl_2 (10 mL), and the reaction mixture was stirred at room temperature for 2 h. Then, the solvent was removed under reduced pressure to give the crude product, which was purified by silica gel flash chromatography using hexane/ethyl acetate (5:1) as eluent to afford compound **7** as a yellow solid in 87% yield. ^{1}H NMR (400 MHz, CD_3COCD_3): δ 7.76 (m, 1H), 7.53 (m, 3H), 7.25 (m, 1H), 7.17 (m, 2H), 6.82 (m, 1H), 6.74 (m, 1H), 6.41 (d, J = 3.2 Hz, 1H), 6.35 (m, 1H), 6.31 (d, J = 16.0 Hz, 1H), 5.55 (d, J = 12.0 Hz, 1H), 4.14 (s, 2H), 3.77 (q, J = 7.2 Hz, 2H), 3.40 (q, J = 7.2 Hz, 4H), 2.56 (m, 2H), 1.70 (s, 6H), 1.56 (m, 2H), 1.30 (m, 2H), 1.21(t, J = 7.2 Hz, 3H), 1.15 (t, J = 7.2 Hz, 6H).

2.6. Synthesis of sensor NRh-Cu

Compound **7** (0.59 g, 1 mmol) and 4-(diethylamino)-2-hydroxybenzaldehyde (0.23 g, 1.2 mmol) were dissolved in ethanol (10 mL) and heated to reflux for 6 h. After removal of ethanol under vacuum, the residue was purified by silica gel flash chromatography using hexane/ethyl acetate (10:1) as eluent to afford compound **NRh-Cu** as a yellow solid in 85% yield. ^{1}H NMR (400 MHz, $CDCl_3$): δ 11.25 (s, 1H), 9.06 (s, 1H), 7.90 (d, J = 4.0 Hz, 1H), 7.51–7.42 (m, 3H), 7.21–7.15 (m, 3H), 6.98 (d, J = 8.0 Hz, 1H), 6.84 (m, 1H), 6.60 (d, J = 8.0 Hz, 1H), 6.46 (d, J = 8.0 Hz, 1H), 6.36 (s, 1H), 6.25 (d, J = 8.0 Hz, 1H), 6.13 (m, 2H), 5.43 (d, J = 12.0 Hz, 1H), 3.67 (q, J = 8.0 Hz, 2H), 3.39 (m, 8H), 2.52

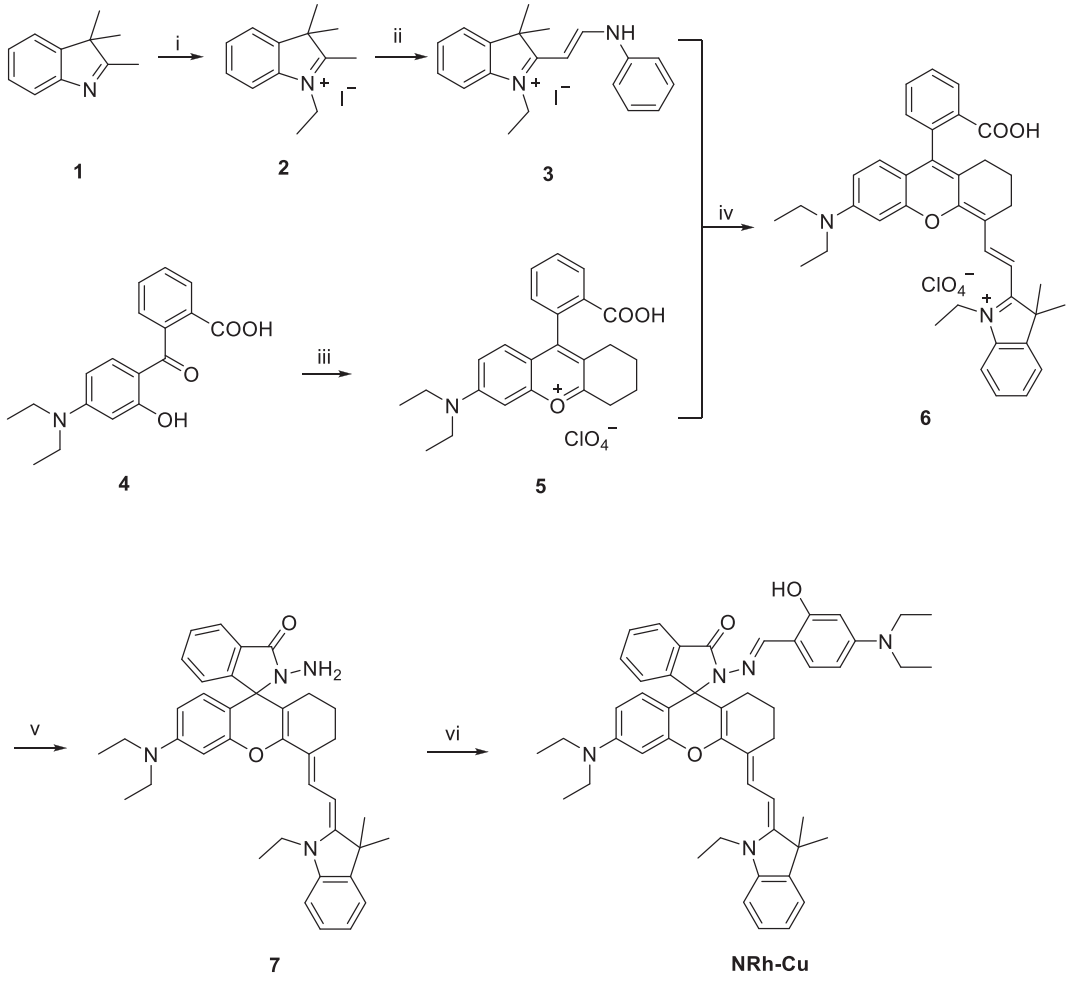

Scheme 1. Synthetic route of **NRh-Cu.**

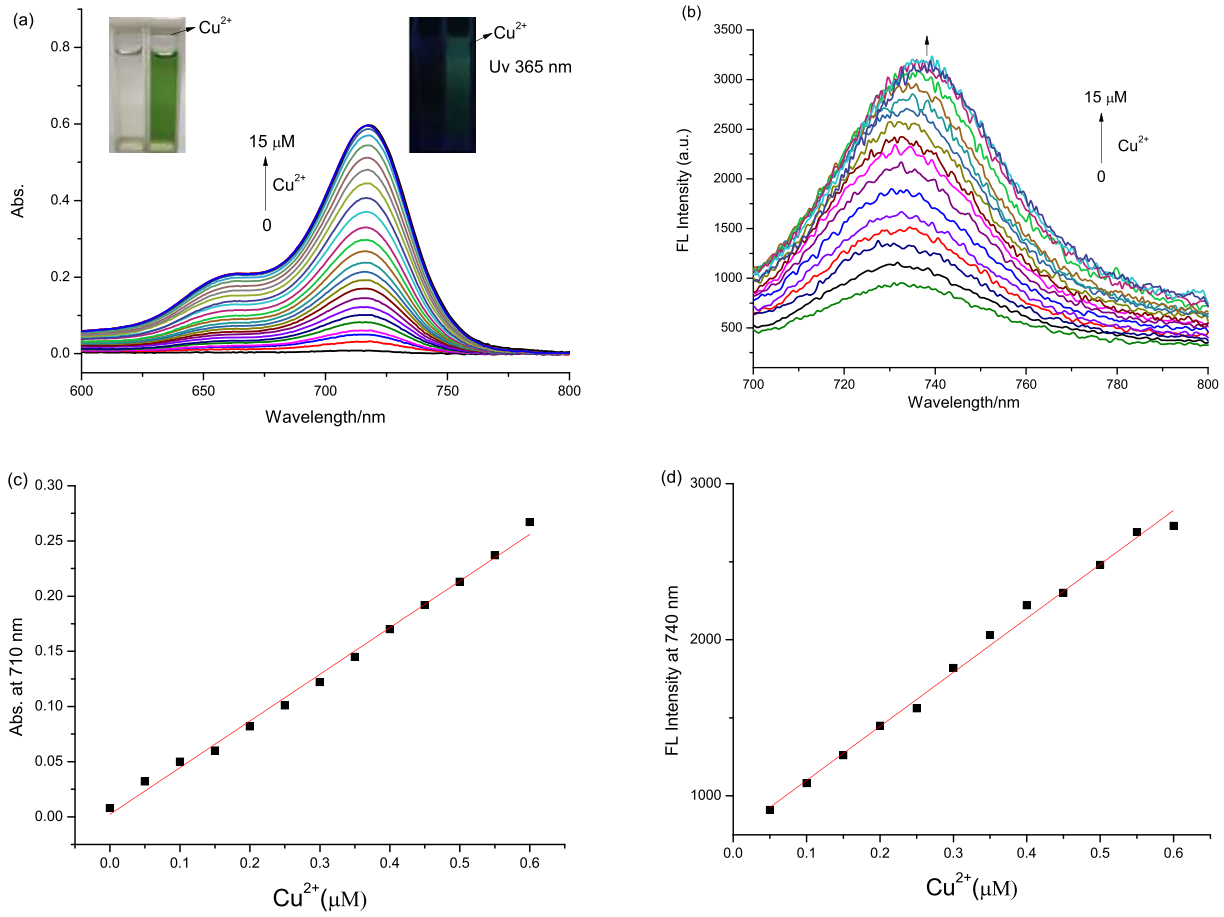

Fig. 1. Changes in the absorption (a) and emission (b) spectra of probe **NRh-Cu** (10 μM) upon the addition of Cu^{2+} from 0 to 15 μM in ethanol/H_2O (1:1 v/v) and the analysis of the absorption (c) and emission (d) detection limit of the probe.

(m, 2H), 1.74 (d, $J = 8.0$ Hz, 4H), 1.59 (m, 8H), 1.23 (t, $J = 7.2$ Hz, 3H), 1.15 (m, 12H). ^{13}C NMR (100 MHz, $CDCl_3$): 164.22, 160.79, 155.89, 154.69, 152.54, 150.50, 149.73, 148.74, 148.00, 144.55, 139.12, 132.90, 128.35, 127.76, 127.68, 123.45, 122.99, 121.61, 120.17, 119.60, 119.11, 108.33, 107.41, 105.58, 103.83, 103.34, 98.22, 97.94, 91.83, 68.13, 445.56, 44.50, 44.28, 36.72, 28.42, 28.33, 25.32, 22.90, 22.22, 12.66, 11.04. MS: m/z calcd for $C_{49}H_{56}N_5O_3$ $[M + H]^+$ 762.4383, found 762.4272.

3. Results and discussion

3.1. Synthesis

The rhodamine hydrazide **7** was prepared according to the previously reported methods with minor modifications (Scheme 1) [14]. Compound **2**, which was easily obtained by alkylation of 2,3,3-trimethyl-3H-indole **1** and ethyl iodide, was converted to the desired intermediate **3** by using *N*,

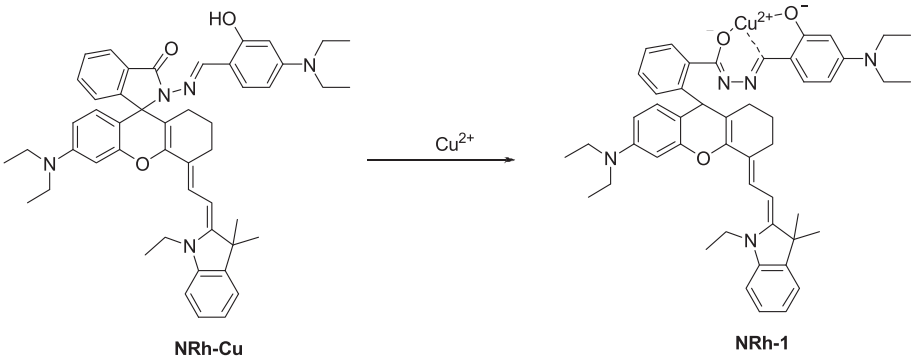

Scheme 2. Proposed mechanism for the off-on sensing of **NRh-Cu** for Cu^{2+}.

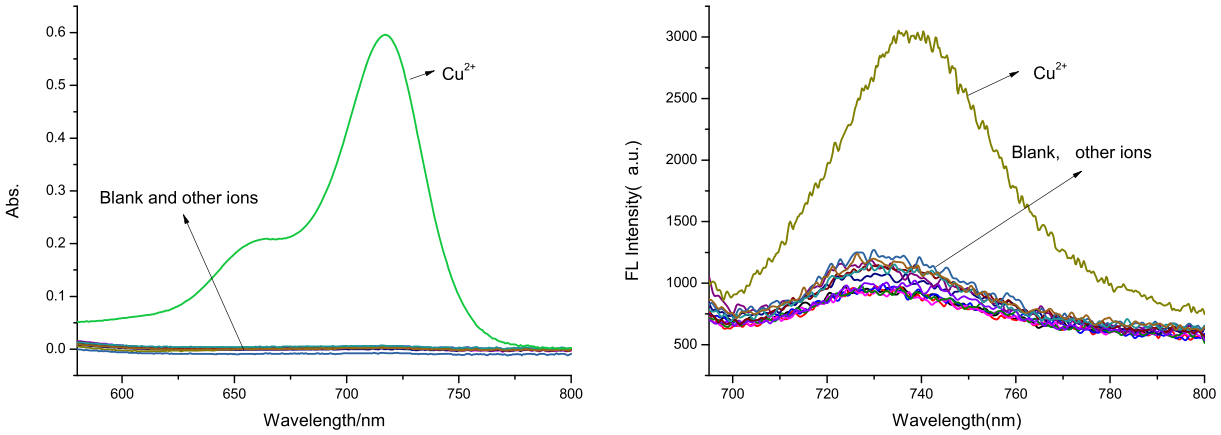

Fig. 2. Absorption and fluorescence spectra of probe (10 μM) in the presence and absence of different metal ions (10 μM) in EtOH-H_2O (1:1, *v*/v).

N′-bis-phenylformamidine in 89% yield. Intermediate **5** was obtained from cyclohexanone and 2-(4-diethylamino-2-hydroxybenzoyl)benzoic acid by a condensation reaction in 90% yield. Compound **7** was conveniently synthesized by condensation of acid **6** with hydrazine hydrate where (benzotriazol-1-yloxy)tripyrrolidino-phosphonium hexafluorophosphate (PyBOP) was used as the coupling reagent. The yield increased to 70%, in comparison with a low yield (≈20%) in the literature method [14]. The probe **NRh-Cu** was synthesized by condensation of rhodamine hydrazide **7** and 4-(diethylamino)-2-hydroxybenzaldehyde. The structure of **NRh-Cu** was characterized by ^{1}H NMR, ^{13}C NMR and HRMS (see the Experimental Section and Supporting Information for details).

3.2. Optical Response of *NRh-Cu* to Cu^{2+}

The spectral response of probe **NRh-Cu** toward Cu^{2+} was investigated in ethanol/H_2O (1:1 v/v) solution. As shown in Fig. S1, **NRh-Cu** displays significant enhancement of fluorescent emission after interacting with Cu^{2+}. To achieve more accurate results, we chose 50% of ethanol as cosolvent. With increasing amounts of Cu^{2+}, the intensity of maximum absorption band at 717 nm was steadily enhanced causing a significant color change in solution (Fig. 1a). These results suggest that **NRh-Cu** could be used as a "naked-eye" probe for Cu^{2+}. Moreover, in the absence of Cu^{2+}, **NRh-Cu** displayed a weak fluorescence emission at 740 nm when excitated at 680 nm. In contrast, **NRh-Cu** showed gradual fluorescence emission enhancement following the addition of increasing concentrations of Cu^{2+} due to the Cu^{2+}-induced ring opening of the spirolactam form (Fig. 1b). The fluorescence intensity at 740 nm has a good linear relationship with Cu^{2+} concentration ranging from 0.1 to 0.6 μM as shown in Fig. 1d and an ultralow detection limit is determined to be 0.95 ppb. In addition, a detection limit of 6.2 ppb is also obtained by absorption spectroscopy (Fig. 1c). The above results indicate that the **NRh-Cu** could serve as an excellent NIR probe for the Cu^{2+} detection.

3.3. Sensing Mechanism

Phenol O, imino N, and carbonyl O atoms were designed to chelate with copper ions. The rhodamine was selected as a signal switcher due to its outstanding properties and a structural change from the spirocyclic state (non-fuorescent) to the ring-open state (fuorescent) induced by metal ions. The probe solution is weakly fluorescent and colorless, indicating that **NRh-Cu** exists in the spirolactam form, which was also supported by the characteristic peak of the 9-carbon of near 68 ppm in the ^{13}C NMR spectrum (Fig. S6). Upon the addition of 1.5 equiv. of Cu^{2+}, the absorbance at 717 nm was obviously enhanced and the probe solution became green and strongly fluorescent, indicating that the ring-opened amide form of **NRh-1** was formed (Scheme 2, Fig. S7, S8).

3.4. Selectivity

A wide range of metal ions such as Li^+, Na^+, K^+, Mg^{2+}, Ca^{2+}, Al^{3+}, Cr^{3+}, Mn^{2+}, Fe^{2+}, Fe^{3+}, Co^{2+}, Ni^{2+}, Zn^{2+}, Cd^{2+}, Ag^+, Pb^{2+}, Sn^{4+}, and Hg^{2+} were selected to investigate the selectivity toward Cu^{2+} (Fig. 2). These results suggest that probe **NRh-Cu** has excellent selectivity toward Cu^{2+} over other metal ions. Moreover, a kinetic study was examined over a 20-min time period. As shown in Fig. 3, Cu^{2+} (2 equiv.) exhibited a rapid turn-on response that reached the maximum emission intensity at 740 nm within 10 min. In contrast, other metal ions were almost nonemissive and stable.

3.5. Practical Applications

In order to check the cytotoxicity of probe **NRh-Cu**, the HeLa cells were incubated for 48 h with varied concentrations of **NRh-Cu** (2–80

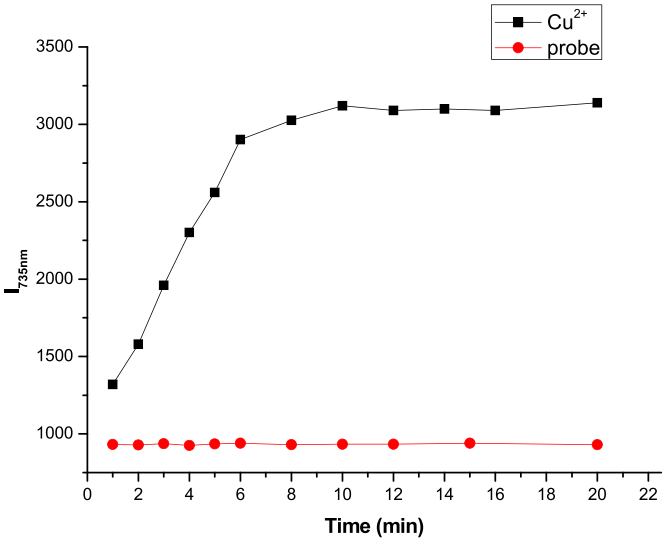

Fig. 3. Time-dependent fluorescence intensity change of probe (λ_{em} = 735 nm, 10 μM) in the presence (blank) and absence of Cu^{2+} (2 equiv) in ethanol/H_2O (v/v = 1:1).

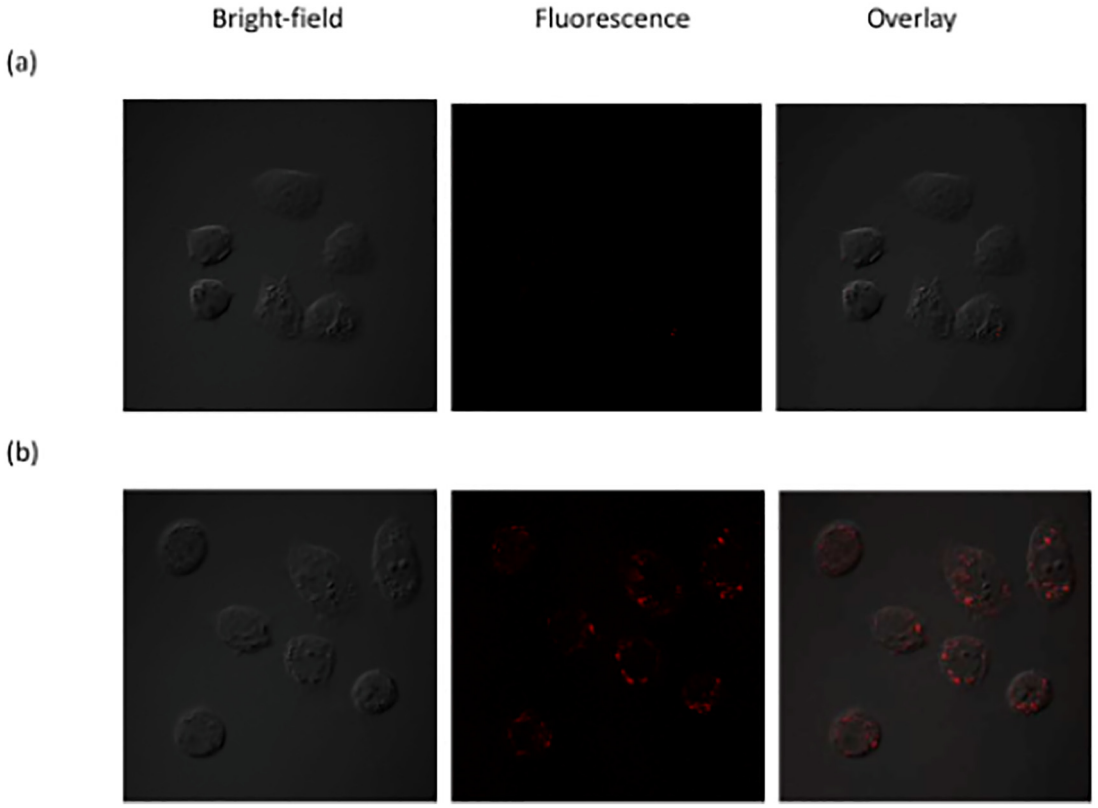

Fig. 4. Fluorescence microscope images of **NRh-Cu** in living HeLa cells. (a) HeLa cells incubated with **NRh-Cu** (10 μM) for 1 h. (b) HeLa cells pretreated with Cu^{2+} (20 μM) for 1 h and followed by incubation with **NRh-Cu** (10 μM) for 30 min.

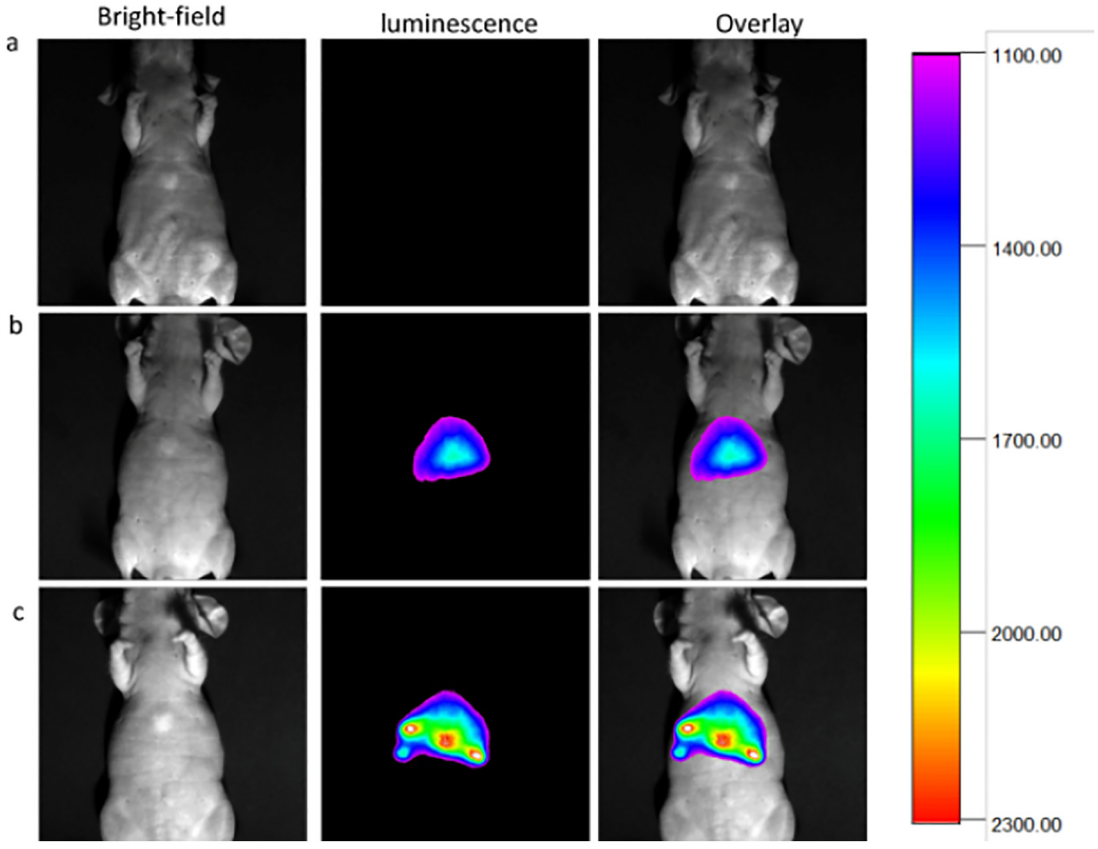

Fig. 5. Fluorescent images of living mice (a) negative control; treated with 0.2 mL of saline (b) negative control; injected with probe **NRh-Cu** (c) preinjected with **NRh-Cu**, and then injected with Cu^{2+}.

μM). However, no significant difference in the proliferation was observed (Fig. S2).

Therefore, the applicability of **NRh-Cu** in the monitoring of intracellular Cu^{2+} was carried out by confocal luminescence microscopy. As shown in Fig. 4a, only a weak emission was observed after incubation with **NRh-Cu** (10 μM) at 37 °C for 1 h. However, a strong enhancement emission was observed under the same conditions when the cells were incubated with 20 μM Cu^{2+} for 1 h at 37 °C and then supplemented with **NRh-Cu** (10 μM). These bioimaging results implied that **NRh-Cu** had good membrane permeability and was potentially suitable for biological application.

Due to the probe's good NIR optical property, the **NRh-Cu** was further untilized to monitor Cu^{2+} in living mice. Male Kunming mice (4 weeks old, ~20 g) were used in the experiments. The mice were injected intravenously with **NRh-Cu** (0.2 mL, 0.2 $mg \cdot mL^{-1}$ in physiological saline). In one experiment, the control group (b) was injected intravenously with physiological saline (0.2 mL). In the other experiment, the group (c) was injected intravenously with Cu^{2+} (0.2 mL, 0.1 mM) in saline. As shown in Fig. 5, the emission intensity increased significantly after treatment with Cu^{2+} (c) as compared with the control treated with normal saline (a) and with **NRh-Cu** (b). The above results implied that the probe **NRh-Cu** may be used to monitor and image Cu^{2+} in the living animals.

4. Conclusion

In summary, a highly selective and sensitive Cu^{2+} NIR probe, **NRh-Cu**, has been developed, and the structure of the probe was characterized by ^1H NMR, ^{13}C NMR and HRMS. The detection limit was calculated to be as low as 0.95 ppb. The sensing mechanism was proposed and confirmed by HRMS spectra. It is noteworthy that the probe could be used for imaging Cu^{2+} *in vitro* and *in vivo*.

Acknowledgements

This work was supported by the Science Foundation of Shandong Province for Excellent Young Scholars (ZR2017JL015) and the Natural Science Foundation of China (21602153).

Appendix A. Supplementary data

Supplementary data to this article can be found online at https://doi.org/10.1016/j.saa.2019.03.062.

References

[1] M.C. Linder, M. Hazegh-Azam, Copper biochemistry and molecular biology, Am. J. Clin. Nutr. 63 (1996) 797–811.
[2] R. Uauy, M. Olivares, M. Gonzalez, Essentiality of copper in humans, Am. J. Clin. Nutr. 67 (1998) 952–959.
[3] L.I. Bruijn, T.M. Miller, D.W. Cleveland, Unraveling the mechanisms involved in motor neuron degeneration in ALS, Annu. Rev. Neurosci. 27 (2004) 723–749.
[4] (a) Y. Liu, Q.Q. Su, M. Chen, Y. Dong, Y.B. Shi, W. Feng, Z.Y. Wu, F.Y. Li, Near-infrared upconversion chemodosimeter for in vivo detection of Cu^{2+} in Wilson disease, Adv. Mater. 28 (2016) 6625–6630;
(b) E.M. Nolan, S.J. Lippard, Tools and tactics for the optical detection of mercuric ion, Chem. Rev. 108 (2008) 3443–3480;
(c) L. Zeng, E.W. Miller, A. Pralle, E.Y. Isacoff, C.J. Chang, A selective turn-on fluorescent sensor for imaging copper in living cells, J. Am. Chem. Soc. 128 (2006) 10–11.
[5] E. Gaggelli, H. Kozlowski, D. Valensin, G. Valensin, Copper homeostasis and neurodegenerative disorders (Alzheimer's, prion, and Parkinson's diseases and amyotrophic lateral sclerosis), Chem. Rev. 106 (2006) 1995–2044.
[6] P. Li, X. Duan, Z.Z. Chen, Y. Liu, T. Xie, L.B. Fang, X.R. Li, M. Yin, B. Tang, A near-infrared fluorescent probe for detecting copper(II) with high selectivity and sensitivity and its biological imaging applications, Chem. Commun. 47 (2011) 7755–7757.
[7] H.R. Yang, C.M. Han, X.J. Zhu, Y. Liu, K.Y. Zhang, S.J. Liu, Q. Zhao, F.Y. Li, W. Huang, Upconversion luminescent chemodosimeter based on NIR organic dye for monitoring methylmercury in vivo, Adv. Funct. Mater. 26 (2016) 1945–1953.
[8] Y.M. Yang, Q. Zhao, W. Feng, F.Y. Li, Luminescent chemodosimeters for bioimaging, Chem. Rev. 113 (2013) 192–270.
[9] (a) J.A.J. Cotruvo, A.T. Aron, K.M. Ramos-Torresa, C.J. Chang, Synthetic fluorescent probes for studying copper in biological systems, Chem. Soc. Rev. 44 (2015) 4400–4414;
(b) V. Dujols, F. Ford, A.W. Czarnik, A long-wavelength fluorescent chemodosimeter selective for Cu(II) ion in water, J. Am. Chem. Soc. 119 (1997) 7386–7387;
(c) X. Zhang, Y. Shiraishi, T. Hirai, Cu(II)-selective green fluorescence of a rhodamine-diacetic acid conjugate, Org. Lett. 9 (2007) 5039–5042;
(d) Y.Q. Ge, R.X. Ji, S.L. Shen, X.Q. Cao, F.Y. Li, A ratiometric fluorescent probe for sensing Cu^{2+} based on new imidazo[1,5-a]pyridine fluorescent dye, Sensors Actuators B Chem. 245 (2017) 875–881;
(e) K.M. Swamy, S.K. Ko, S.K. Kwon, H.N. Lee, C. Mao, J.M. Kim, K.H. Lee, J.H. Kim, I. Shin, J.Y. Yoon, Boronic acid-linked fluorescent and colorimetric probes for copper ions, Chem. Commun. 44 (2008) 5915–5917;
(f) Y.Q. Ge, X.L. Zheng, R.X. Ji, S.L. Shen, X.Q. Cao, A new pyrido[1,2-a]benzimidazole-rhodamine FRET system as an efficient ratiometric fluorescent probe for Cu^{2+} in living cells, Anal. Chim. Acta 965 (2017) 103–110;
(g) X.L. Zheng, R.X. Ji, X.Q. Cao, Y.Q. Ge, FRET-based ratiometric fluorescent probe for Cu^{2+} with a new indolizine fluorophore, Anal. Chim. Acta 978 (2017) 48–54;
(h) N.R. Chereddy, S. Thennarasu, Synthesis of a highly selective bis-rhodamine chemosensor for naked-eye detection of Cu^{2+} ions and its application in bioimaging, Dyes Pigments 91 (2011) 378–382;
(i) X. Qi, E.J. Jun, L. Xu, S.J. Kim, J.S.J. Hong, Y.J. Yoon, J. Yoon, New BODIPY derivatives as OFF-ON fluorescent chemosensor and fluorescent chemodosimeter for Cu^{2+}: cooperative selectivity enhancement toward Cu^{2+}, J. Org. Chem. 71 (2006) 2881–2884;
(j) N. Li, Y. Xiang, A.J. Tong, Highly sensitive and selective "turn-on" fluorescent chemodosimeter for Cu^{2+} in water via Cu^{2+}-promoted hydrolysis of lactone moiety in coumarin, Chem. Commun. 46 (2010) 3363–3365;
(k) S.H. Mashraqui, K. Poonia, R. Betkar, M. Chandiramani, A novel retro-reaction strategy toward designing a selective fluorescence Cu(II) chemodosimeter, Tetrahedron Lett. 51 (2010) 4336–4339;
(l) D.P. Wang, Y. Shiraishi, T. Hirai, A BODIPY-based fluorescent chemodosimeter for Cu(II) driven by an oxidative dehydrogenation mechanism, Chem. Commun. 47 (2011) 2673–2675;
(m) L. Yuan, W.Y. Lin, Z.M. Cao, L.L. Long, J.Z. Song, Photocontrollable analyte-responsive fluorescent probes: a photocaged copper-responsive fluorescence turn-on probe, Chem. Eur. J. 17 (2011) 689–696;
(n) C.W. Yu, T. Wang, K. Xu, J. Zhao, M. Li, S. Weng, J. Zhang, Characterization of a highly Cu^{2+}-selective fluorescent probe derived from rhodamine B, Dyes Pigments 96 (2013) 38–44;
(o) C. Kar, M.D. Adhikari, A. Ramesh, G. Das, NIR-and FRET-based sensing of Cu^{2+} and S^{2-} in physiological conditions and in live cells, Inorg. Chem. 52 (2013) 743–752;
(p) S.K. Sahoo, D. Sharma, A. Moirangthem, A. Kuba, R. Thomas, R. Kumar, A. Kuwar, H.J. Choi, A. Basu, Pyridoxal derived chemosensor for chromogenic sensing of Cu^{2+} and fluorogenic sensing of Fe^{3+} in semi-aqueous medium, J. Lumin. 172 (2016) 297–303;
(q) U.A. Fegade, S.K. Sahoo, A. Singh, N. Singh, S.B. Attarde, A.S. Kuwar, A chemosensor showing discriminating fluorescent response for highly selective and nanomolar detection of Cu^{2+} and Zn^{2+} and its application in molecular logic gate, Anal. Chim. Acta 872 (2015) 63–69;
(r) A. Kuwar, R. Patil, A. Singh, S.K. Sahoo, J. Marek, N. Singh, A two-in-one dual channel chemosensor for Fe^{3+} and Cu^{2+} with nanomolar detection mimicking the logic gate, J. Mater. Chem. C 3 (2015) 453–460;
(s) D. Sharma, A. Kuba, R. Thomas, R. Kumar, H.J. Choi, S.K. Sahoo, An aqueous friendly chemosensor derived from vitamin B6 cofactor for colorimetric sensing of Cu^{2+} and fluorescent turn-off sensing of Fe^{3+}, Spectrochim. Acta A 153 (2016) 393–396;
(t) Y. Xiang, A. Tong, P. Jin, Y. Ju, New fluorescent rhodamine hydrazone chemosensor for Cu(II) with high selectivity and sensitivity, Org. Lett. 8 (2006) 2863–2866;
(u) Y. Fang, Y. Zhou, Q. Rui, C. Yao, Rhodamine-ferrocene conjugate chemosensor for selectively sensing copper(II) with multisignals: chromaticity, fluorescence, and electrochemistry and its application in living cell imaging, Organometallics 34 (2015) 2962–2970;
(v) H.N. Kim, M.H. Lee, H.J. Kim, J.S. Kim, A new trend in rhodamine-based chemosensors: application of spirolactam ring-opening to sensing ions, Chem. Soc. Rev. 37 (2008) 1465–1472;
(w) P. Aguirre, O. García-Beltrán, V. Tapia, Y. Muñoz, B.K. Cassels, M.T. Núñez, Neuroprotective effect of a new 7,8-dihydroxycoumarin-based Fe^{2+}/Cu^{2+} chelator in cell and animal models of Parkinson's disease, ACS Chem. Neurosci. 8 (2017) 178–185;
(x) B. Muthuraj, S. Layek, S.N. Balaji, V. Trivedi, P.K. Iyer, Multiple function fluorescein probe performs metal chelation, disaggregation, and modulation of aggregated Aβ and Aβ-Cu complex, ACS Chem. Neurosci. 6 (2015) 1880–1891;
(y) H. Zhang, X. Dong, Y. Sun, Carnosine-LVFFARK-NH2 conjugate: a moderate chelator but potent inhibitor of Cu^{2+}-mediated amyloid β-protein aggregation, ACS Chem. Neurosci. 9 (2018) 2689–2700.
[10] (a) T. Hirayamaa, G.C. Van de Bittnera, L.W. Grayb, S. Lutsenkob, C.J. Chang, Near-infrared fluorescent sensor for in vivo copper imaging in a murine Wilson disease model, PNAS. 109 (2012) 2228–2233;
(b) F. Lv, X. Feng, H. Tang, L. Liu, Q. Yang, S. Wang, Development of film sensors based on conjugated polymers for copper (II) ion detection, Adv. Funct. Mater. 21 (2011) 845–850;

(c) B. Muthuraj, R. Deshmukh, V. Trivedi, P.K. Iyer, Highly selective probe detects Cu^{2+} and endogenous NO gas in living cell, ACS Appl. Mater. Interfaces 6 (2014) 6562–6569;
(d) G. Saikia, A.K. Dwivedi, P.K. Iyer, Development of solution, film and membrane based fluorescent sensor for the detection of fluoride anions from water, Anal. Methods 4 (2012) 3180–3186;
(e) A.H. Malik, S. Hussain, A.S. Tanwar, S. Layek, V. Trivedi, P.K. Iyer, An anionic conjugated polymer as a multi-action sensor for the sensitive detection of Cu^{2+} and PPi, real-time ALP assaying and cell imaging, Analyst 140 (2015) 4388–4392;
(f) X. Zhao, Y. Liu, K.S. Schanze, A conjugated polyelectrolyte-based fluorescence sensor for pyrophosphate, Chem. Commun. (2007) 2914–2916;
(g) G. Jágerszki, A. Grün, I. Bitter, K. Töth, R.E. Gyurcsányi, Ionophore-gold nanoparticle conjugates for Ag^{+}-selective sensors with nanomolar detection limit, Chem. Commun. 46 (2010) 607–609;
(h) Y. Bao, H. Wang, Q. Li, B. Liu, Q. Li, W. Bai, B. Jin, R. Bai, 2,2-Biimidazole-based conjugated polymers as a novel fluorescent sensing platform for pyrophosphate anion, Macromolecules 45 (2012) 3394–3401.
[11] L. Yuan, W.Y. Lin, K.B. Zheng, L.W. He, W.M. Huang, Far-red to near infrared analyte-responsive fluorescent probes based on organic fluorophore platforms for fluorescence imaging, Chem. Soc. Rev. 42 (2013) 622–661.
[12] Z.Q. Guo, S. Park, J. Yoon, I. Shin, Recent progress in the development of near-infrared fluorescent probes for bioimaging applications, Chem. Soc. Rev. 43 (2014) 16–29.
[13] M. Marena, Near-infrared spectroscopy and hyperspectral imaging: non- destructive analysis of biological materials, Chem. Soc. Rev. 43 (2014) 8200–8214.
[14] L. Yuan, W.Y. Lin, Y.T. Yang, H. Chen, A unique class of near-infrared functional fluorescent dyes with carboxylic-aid-modulated fluorescence ON/OFF switching: rational design, synthesis, optical properties, theoretical calculations, and applications for fluorescence imaging in living animals, J. Am. Chem. Soc. 134 (2012) 1200–1211.